

Divya Mathur,<sup>a</sup> Kanchan Anand,<sup>b</sup> Deepika Mathur,<sup>a</sup> Nirmala Jagadish,<sup>c</sup> Anil Suri<sup>c</sup> and Lalit C. Garg<sup>a\*</sup>

<sup>a</sup>Gene Regulation Laboratory, National Institute of Immunology, New Delhi 110067, India,

<sup>b</sup>European Molecular Biology Laboratory, Structural and Computational Biology Unit, Meyerhofstrasse 1, 69117 Heidelberg, Germany, and <sup>c</sup>Genes and Proteins Laboratory, National Institute of Immunology, New Delhi 110067, India

Correspondence e-mail:  
lalit@nii.res.in, lalitcarg@yahoo.com

Received 19 December 2006  
Accepted 20 March 2007

## Crystallization and preliminary X-ray characterization of phosphoglucose isomerase from *Mycobacterium tuberculosis* H37Rv

Phosphoglucose isomerase is a ubiquitous enzyme that catalyzes the isomerization of D-glucopyranose-6-phosphate to D-fructofuranose-6-phosphate. The present investigation reports the expression, purification, crystallization and preliminary crystallographic studies of the phosphoglucose isomerase from *Mycobacterium tuberculosis* H37Rv, which shares 46% sequence identity with that of its human host. The recombinant protein, which was prepared using an *Escherichia coli* expression system, was crystallized by the hanging-drop vapour-diffusion method. The crystals diffracted to a resolution of 2.8 Å and belonged to the orthorhombic space group  $I2_12_12_1$ , with unit-cell parameters  $a = 109.0$ ,  $b = 119.8$ ,  $c = 138.9$  Å.

### 1. Introduction

*Mycobacterium tuberculosis*, the causative agent of tuberculosis, is one of the leading causes of death in humans. The recent emergence of multidrug-resistant strains and a global increase in the number of cases of tuberculosis has necessitated the search for new drugs (Murray & Salomon, 1998). The enzymes that are crucial for the growth and survival of the infectious agent within the host cell can be targeted for potentially effective drug design. During mycobacterium infection in macrophages, a metabolic shift from a strict aerobic respiratory mode to anaerobic metabolism occurs, with a significant increase in the levels of glycolytic enzymes. During this stage, 70% of the organism's energy is derived from glycolysis (Jayanthi *et al.*, 1975). Thus, being central to the organism's survival, the enzymes involved in glycolysis present an attractive alternate target for drug design against *M. tuberculosis*.

Phosphoglucose isomerase (PGI; EC 5.3.1.9) is a multifunctional protein that plays a central role in the glycolysis and gluconeogenesis pathways. It catalyzes the reversible isomerization of D-glucopyranose-6-phosphate to D-fructofuranose-6-phosphate. This isomerization step is a vital link between the Embden–Meyerhoff–Parnas, Entner–Duodoroff and pentose phosphate pathways. In addition, PGI has been reported to function as an autocrine motility factor, as a neuroleukin and as a serine proteinase inhibitor (Chaput *et al.*, 1988; Faik *et al.*, 1988; Watanabe *et al.*, 1991, 1996; Cao *et al.*, 2000).

PGIs from a number of species have been cloned and characterized (Froman *et al.*, 1989; Marchand *et al.*, 1989; Goffrini *et al.*, 1991; Tuckman *et al.*, 1997; Katz, 1997; Kao & Lee, 2002; Richards, 2004; Rudolph *et al.*, 2004). It has been shown that while the catalytic domain remains conserved across species, significant differences exist outside the catalytic domain that are reflected in structural differences between PGIs from different species. The crystal structures of PGI from a number of species have revealed that although the enzymes from different species have a similar overall fold, they exhibit significant structural differences (Sun *et al.*, 1999; Chou *et al.*, 2000; Jeffery *et al.*, 2001; Davies & Muirhead, 2002, 2003; Graham Solomons *et al.*, 2004). For example, the *Leishmania mexicana* and human PGIs share 58% identity and have conserved substrate-binding residues. A comparison of the crystal structures of the two enzymes shows that although they both present the same overall fold,



© 2007 International Union of Crystallography  
All rights reserved

the small domain of the PGI from *L. mexicana* differs significantly from that of the human PGI. The parasitic PGI has a more open conformation and a larger active site compared with that of human (Cordeiro, Hardre *et al.*, 2004; Cordeiro, Michels *et al.*, 2004). These investigators proposed that the larger cavity of the parasite enzyme may be used for the design of inhibitors of the parasite enzyme that are too large to fit into the catalytic site of the mammalian PGI. The structural and sequence differences between glycolytic enzymes such as aldolase, triose phosphate isomerase and glyceraldehyde-3-phosphate dehydrogenase (GAPDH) between *Trypanosoma brucei* and *T. cruzi* and their human host have been successfully exploited to design effective inhibitors of the enzymes of the pathogen that have no effect on their mammalian counterparts (Verlinde *et al.*, 1992; Aronov *et al.*, 1999; Verlinde *et al.*, 2001, 2002).

Since the *M. tuberculosis* and human PGIs share only ~46% identity and their amino-acid sequences differ significantly outside the catalytic domain (Mathur *et al.*, 2005), their crystal structures may reveal certain characteristics unique to *M. tuberculosis* PGI that may possibly be exploited for effective drug design against the PGI of the pathogen. Here, we describe the expression, purification, crystallization and X-ray diffraction analysis of recombinant PGI from *M. tuberculosis*.

## 2. Experimental procedures

### 2.1. Expression and purification

The gene encoding PGI from *M. tuberculosis* H37Rv was PCR-amplified using gene-specific primers from the BAC genomic DNA library and cloned into the pET22b(+) vector in *Nde*I and *Xho*I sites, which added sequences encoding a six-histidine tag at the C-terminus (Mathur & Garg, 2007). *Escherichia coli* BL21 (DE3) cells harbouring the resultant recombinant plasmid were induced at  $A_{600} = 0.5$  with 1 mM IPTG and grown for a further 8 h at 310 K. Cells were harvested by centrifugation at 4500g for 5 min. The pelleted cells were resuspended in sonication buffer (50 mM  $\text{NaH}_2\text{PO}_4$ , 300 mM NaCl pH 7.8) and lysed by sonication (30 cycles of 1 min pulse on followed by 30 s pulse off). The sonication supernatant obtained by centrifugation of the lysate at 12 000g for 20 min at 277 K was mixed with  $\text{Ni}^{2+}$ -NTA agarose beads (Qiagen, Germany).



**Figure 1**  
A bipyramidal crystal of PGI from *M. tuberculosis* with dimensions of  $0.3 \times 0.2 \times 0.15$  mm.

Binding of the His-tagged recombinant PGI to the  $\text{Ni}^{2+}$ -NTA agarose took place for 1 h with end-to-end shaking. Following the addition of  $\text{Ni}^{2+}$ -NTA agarose beads, a centrifugation step was performed at 1200g in a swinging-bucket rotor for 2 min. The flowthrough was discarded and nonspecifically bound proteins were removed by washing the beads twice in 15 ml Tris-phosphate buffer (0.01 M Tris, 0.1 M sodium dihydrogen phosphate pH 7.8). The recombinant protein was eluted with 12.5 ml of 250 mM imidazole (in Tris-phosphate buffer pH 7.8).

### 2.2. Crystallization

For crystallization, the purified His-tagged recombinant PGI of *M. tuberculosis* was concentrated to  $10 \text{ mg ml}^{-1}$  in a solution consisting of 100 mM NaCl and 50 mM Tris-HCl pH 7.4. Initial crystals were obtained using the hanging-drop vapour-diffusion method. The initial drops were a 1:1 mixture of protein solution and reservoir solution containing 1.5 M ammonium sulfate and 0.1 M HEPES pH 7.5 at 288 K. The clusters of small crystals that appeared over the next 48 h were optimized by microseeding. A few crystals were transferred to 50  $\mu\text{l}$  precipitant solution and mechanically crushed by pipetting and vortexing. This resulting seed solution was then diluted tenfold to 10 000-fold. Simultaneously, the concentration of the reservoir solution was lowered and the pH of the buffer was increased to 8.0 to slow the process of supersaturation. Droplets contained 1.5  $\mu\text{l}$  protein solution, 1.5  $\mu\text{l}$  reservoir solution (containing 1.26 M ammonium sulfate and 0.1 M HEPES pH 8.0) and 0.4  $\mu\text{l}$  seed solution and were equilibrated against 500  $\mu\text{l}$  precipitant solution in a hanging-drop setup.

## 3. Results and discussion

On induction, recombinant PGI accumulated in the cells in both a soluble form and as inclusion bodies. The recombinant His-tagged

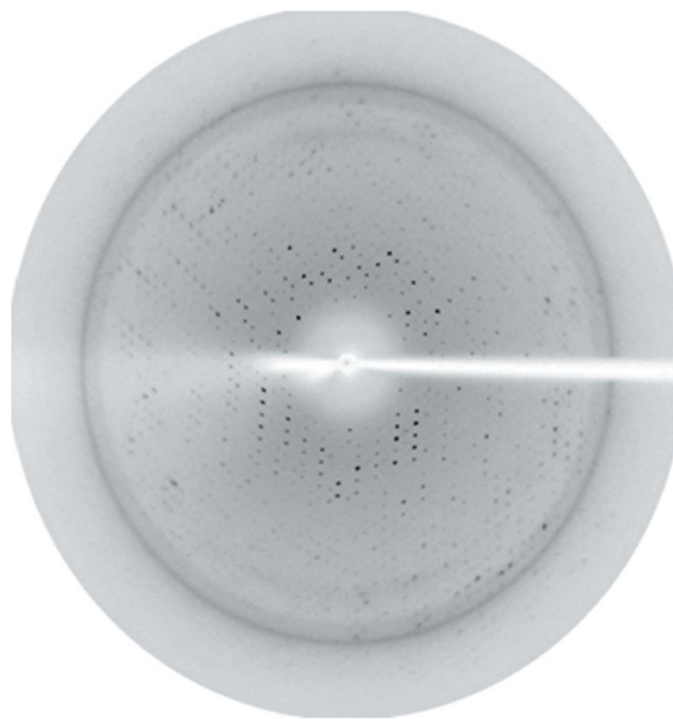


**Figure 2**  
A diffraction pattern of a PGI crystal collected at beamline ID23-1 at the ESRF Grenoble, France with exposure times adjusted to avoid incomplete data arising from overloading.

**Table 1**X-ray data-collection statistics for recombinant PGI from *M. tuberculosis*.

Values in parentheses are for the highest resolution shell.

Beamline	ESRF ID23
Detector	ADSC Q105 CCD
Space group	$I2_12_12_1$
Wavelength (Å)	0.9761
Resolution (Å)	2.8 (2.85–2.80)
Total No. of reflections	100147
No. of unique reflections	22359
Completeness (%)	98.2 (99.5)
Mosaicity (°)	0.045
$R_{\text{meas}}^\dagger$ (%)	9.6 (43.8)
$R_{\text{merge}}^\ddagger$ (%)	17.5 (55.5)
Redundancy	4.5 (4.5)
$I/\sigma(I)$	11.88 (3.45)
Unit-cell parameters (Å)	$a = 109.0, b = 119.8, c = 138.9$

$^\dagger R_{\text{meas}}$  is the redundancy-independent  $R$  factor on intensities.  $^\ddagger R_{\text{merge}} = 100 \times \sum_i |\sum_j |I(h)_i - I(h)_j| / \sum_j I(h)_j$ , where  $I(h)_i$  is the  $i$ th observation of reflection  $h$  and  $\langle I(h) \rangle$  is the mean intensity of all observations of  $h$ .

PGI was purified from the soluble fraction by single-step Ni–NTA affinity chromatography and used for crystallization. The native molecular weight of the purified protein was determined to be ~120 kDa by gel-filtration chromatography, whereas it appeared as a single band of approximately 61 kDa on SDS–PAGE gels, indicating its homodimeric nature (Mathur *et al.*, 2005).

The bipyramidal crystals grew to dimensions of  $0.3 \times 0.2 \times 0.15$  mm in about a week (Fig. 1). The crystals were directly flash-cooled at 100 K in a stream of nitrogen gas for data collection. Initially, the optimum-sized crystals diffracted poorly to about  $10 \text{ \AA}$ . Collecting data from these crystals at room temperature did not improve the diffraction. A series of cryoprotectants were tried to attempt improve the diffraction and finally the post-crystallization treatment described by Heras & Martin (2005), using a stepwise increasing concentration of glycerol, helped to achieve diffraction to  $2.8 \text{ \AA}$ . Crystals soaked overnight in 20% glycerol showed no significant radiation damage during data collection. X-ray diffraction data sets were collected using a single crystal with  $1^\circ$  oscillation steps over a range of  $180^\circ$  (Fig. 2). In order to reduce radiation damage and to collect a complete data set, the transmission dose was checked stepwise from 0% to a final transmission dose of 25% with a 1 s exposure per frame at the ID23-1 beamline of the ESRF (Grenoble, France) using an ADSC Quantum Q105 CCD detector at a wavelength of  $0.9761 \text{ \AA}$  (Table 1).

The data were integrated and scaled using *XDS* (Kabsch, 1993). The overall  $R_{\text{meas}}$ , a redundancy-independent  $R$  factor, was 9.6%. The data were complete to 98.2% and revealed the crystals to belong to the orthorhombic space group  $I2_12_12_1$ , with unit-cell parameters  $a = 109.0, b = 119.8, c = 138.9 \text{ \AA}$ . The crystals were found to have a high solvent content of 67% (a Matthews coefficient of  $3.4 \text{ \AA}^3 \text{ Da}^{-1}$ ). The asymmetric unit contained one molecule of PGI. The data-collection and processing statistics are summarized in Table 1. The structure was solved by the molecular-replacement method (Crowther, 1972) employing the *Phaser* program (Storoni *et al.*, 2004) using PGI from rabbit (PDB code 1xtb) as a search model. We are currently in the process of refining the structure.

Financial support from the Department of Biotechnology, India is acknowledged. We thank the beamline (ID23-1) staff at the ESRF (Grenoble, France) for their kind help with data collection.

## References

- Aronov, A. M., Suresh, S., Buckner, F. S., Van Voorhis, W. C., Verlinde, C. L. M. J., Opperdoes, F. R., Hol, W. G. J. & Gelb, M. H. (1999). *Proc. Natl Acad. Sci. USA*, **96**, 4273–4278.
- Cao, M. J., Osatomi, K., Matsuda, R., Ohkubo, M., Hara, K. & Ishihara, T. (2000). *Biochem. Biophys. Res. Commun.* **272**, 485–489.
- Chaput, M., Claes, V., Portetelle, D., Cludts, I., Cravador, A., Burny, A., Gras, H. & Tartar, A. (1988). *Nature (London)*, **332**, 454–455.
- Chou, C. C., Sun, Y. J., Meng, M. & Hsiao, C. D. (2000). *J. Biol. Chem.* **275**, 23154–23160.
- Cordeiro, A. T., Hardre, R., Michels, P. A., Salmon, L., Delboni, L. F. & Thiemann, O. H. (2004). *Acta Cryst. D* **60**, 915–919.
- Cordeiro, A. T., Michels, P. A. M., Delboni, L. F. & Thiemann, O. H. (2004). *Eur. J. Biochem.* **271**, 2765–2772.
- Crowther, R. A. (1972). *The Molecular Replacement Method*, edited by M. G. Rossmann, pp. 173–178. New York: Gordon & Breach.
- Davies, C. & Muirhead, H. (2002). *Proteins*, **49**, 577–579.
- Davies, C. & Muirhead, H. (2003). *Acta Cryst. D* **59**, 453–465.
- Faik, P., Walker, J. I., Redmill, A. A. & Morgan, M. J. (1988). *Nature (London)*, **332**, 455–457.
- Froman, B. E., Tait, R. C. & Gottlieb, L. D. (1989). *Mol. Gen. Genet.* **217**, 126–131.
- Goffrini, P., Wesolowski-Louvel, M. & Ferrero, I. (1991). *Mol. Gen. Genet.* **228**, 401–409.
- Graham Solomons, J. T., Zimmerly, E. M., Burns, S., Krishnamurthy, N., Swan, M. K., Krings, S., Muirhead, H., Chirgwin, J. & Davies, C. (2004). *J. Mol. Biol.* **342**, 847–860.
- Heras, B. & Martin, J. L. (2005). *Acta Cryst. D* **61**, 1173–1180.
- Jayanthi, B. N., Ramachandra, P. M., Suryanarayana, M. P. & Venkatasubramanian, T. A. (1975). *Can. J. Microbiol.* **21**, 1688–1691.
- Jeffery, C. J., Hardre, R. & Salmon, L. (2001). *Biochemistry*, **40**, 1560–1566.
- Kabsch, W. (1993). *J. Appl. Cryst.* **26**, 795–800.
- Kao, H. W. & Lee, S. C. (2002). *Mol. Biol. Evol.* **19**, 367–374.
- Katz, L. A. (1997). *Insect Mol. Biol.* **6**, 305–318.
- Marchand, M., Kooystra, U., Wierenga, R. K., Lambeir, A. M., Van Beeumen, J., Opperdoes, F. R. & Michels, P. A. (1989). *Eur. J. Biochem.* **184**, 455–464.
- Mathur, D., Ahsan, Z., Tiwari, M. & Garg, L. C. (2005). *Biochem. Biophys. Res. Commun.* **337**, 626–632.
- Mathur, D. & Garg, L. C. (2007). *Protein Expr. Purif.* **52**, 373–378.
- Murray, C. J. & Salomon, J. A. (1998). *Proc. Natl Acad. Sci. USA*, **95**, 13881–13886.
- Richards, G. P. (2004). *Biochim. Biophys. Acta*, **1702**, 89–102.
- Rudolph, B., Hansen, T. & Schonheit, P. (2004). *Arch. Microbiol.* **181**, 82–87.
- Storoni, L. C., McCoy, A. J. & Read, R. J. (2004). *Acta Cryst. D* **60**, 432–438.
- Sun, Y. J., Chou, C. C., Chen, W. S., Wu, R. T., Meng, M. & Hsiao, C. D. (1999). *Proc. Natl Acad. Sci. USA*, **96**, 5412–5417.
- Tuckman, D., Donnelly, R. J., Zhao, F. X., Jacobs, W. R. Jr & Connell, N. D. (1997). *J. Bacteriol.* **179**, 2724–2730.
- Verlinde, C. L. M. J., Bressi, J. C., Choe, J., Suresh, S., Buckner, F. S., Van Voorhis, W. C., Michels, P. A. M., Gelb, M. H. & Hol, W. G. J. (2002). *J. Braz. Chem. Soc.* **13**, 843–848.
- Verlinde, C. L. M. J., Hannaert, V., Blonski, C., Willson, M., Périé, J. J., Fothergill-Gilmore, L. A., Opperdoes, F. R., Gelb, M. H., Hol, W. G. J. & Michels, P. A. M. (2001). *Drug Resist. Updat.* **4**, 50–65.
- Verlinde, C. L. M. J., Witmans, C. J., Pijning, T., Kalk, K. H., Hol, W. G. J. & Opperdoes, F. R. (1992). *Protein Sci.* **1**, 1578–1584.
- Watanabe, H., Carmi, P., Hogan, V., Raz, T., Silletti, S., Nabi, I. R. & Raz, A. (1991). *J. Biol. Chem.* **266**, 13442–13448.
- Watanabe, H., Takehana, K., Date, M., Shinozaki, T. & Raz, A. (1996). *Cancer Res.* **56**, 2960–2963.